

# System based Code Evaluation Criteria for CDM Applications in Sensor and Data Transmission Systems

Peter Stapf<sup>1</sup>, Marek Götten<sup>1,2</sup><sup>a</sup>, Andreas Ahrens<sup>1</sup><sup>b</sup> and Steffen Lochmann<sup>1</sup><sup>c</sup>

<sup>1</sup>*Bereich Elektrotechnik und Informatik, Hochschule Wismar,*

*University of Technology Business and Design, Philipp-Müller-Straße 14, 23966 Wismar, Germany*

<sup>2</sup>*Escuela Técnica Superior de Ingeniería y Sistemas de Telecomunicación, Universidad Politécnica de Madrid, Technical University of Madrid, Crtra de Valenica, km 7, Madrid, Spain*

**Keywords:** Code-division Multiplex, Fibre Bragg Gratings, Optical Sensors, Binary Sequences.

**Abstract:** To increase the multiplexing capability of code-division multiplexing (CDM) applied in optical sensor networks, a system based code evaluation is required. This contribution analyses evaluation criteria for sequences applied in CDM systems. A comparison of an optical sensor application and a single user data transmission system is presented. While a detection signal-to-noise ratio and the bit error rate are used to evaluate data transmission systems, the proposed optical sensor application uses a modified signal-to-multiuser-interference ratio (mSMUI). The main difference exists in the handling of interference. In contrary to data transmission, the mSMUI requires a separation of positive and negative interferences. Both applications are simulated for different binary sequences. While the Legendre sequence with a length of 503 chips achieves the over all best results for the optical sensor application, the single user data transmission simulation shows no significant sequence influence.

## 1 INTRODUCTION

Optical sensors, such as fibre-Bragg gratings (FBGs), gained increased recognition due to their preferable attributes (Jelbuldina et al., 2018), (Presti et al., 2019). They are light, small, are immune to an electromagnetic environment and can be used together with already known multiplexing techniques (Rajan, 2015). These can include wavelength-division multiplexing (WDM), code-division multiplexing (CDM), time-division multiplexing (TDM), frequency shifted interferometry (FSI) and optical frequency domain refractometry (OFDR) (Götten et al., 2020), (Wang et al., 2012), (Ou et al., 2017), (Kaplan et al., 2019). Especially CDM increases the amount of FBGs that can be evaluated in one sensor system to multiple thousand sensors within a single fibre (Götten et al., 2020). This allows detailed health monitoring covering a whole smart structure with dense spatial resolution (Braghin et al., 2013), (Nawrot et al., 2017).

With the introduction of code-division multiple access (CDMA) in a third generation communica-

tion system the common correlation receiver and the RAKE receiver are very popular receiver designs (Lim et al., 2006). The correlation receiver optimizes the signal-to-noise ratio (SNR), if only white noise superimposes the signals at the receiver input. The Rake receiver is a special receiver for radio channels with multipath propagation and in systems with direct sequence spreading. It consists of several correlators according to the number of propagation paths (Price and Green, 1958).

This work focusses on the evaluation of quality criteria with regard to their applicability in system optimization. In data transmission the detection SNR, as the argument of the complement error function, has proven to be a suitable criterion when optimizing data transmission systems. The transferability to sensor-based systems has not yet been investigated. Section 2 explains the concept of CDM in optical sensor systems. A comparison of system based code evaluation criteria is shown in Section 3. In Section 4 a simulation of a CDM interrogated optical sensor system is introduced. A single user data transmission simulation is proposed and analysed in Section 5. Both simulations examine selected binary sequences, including Gold-, Legendre-, M- and random sequences. A

<sup>a</sup>  <https://orcid.org/0000-0001-5032-5776>

<sup>b</sup>  <https://orcid.org/0000-0002-7664-9450>

<sup>c</sup>  <https://orcid.org/0000-0002-0938-2186>

conclusion is given in Section 6.

## 2 SENSOR SYSTEM CONCEPT

A serial fibre optical sensor network can be interrogated as depicted in Figure 1. A broadband light source provides light for the FBGs to reflect. A modulator applies a sequence consisting of '1s' and '0s'. The '1s' and '0s' represent light turned on and off. After the reflection at the FBGs, the light is split into two paths, where each reflected sequence is again modulated. The first (direct) path uses the same sequence, while the second (inverted) path modulates the inverted sequence. The modulators are driven with a specific time delay, which defines the interrogated FBG. A spectrometer collects the light after the corresponding modulation step. The inverted path spectrum is then subtracted from the direct path spectrum which corresponds to sequence inverted keying (SIK). This results in a difference spectrum. The corresponding peak wavelength of the chosen FBG can be detected and evaluated. The set up can be further expanded by using WDM, with the inclusion of multiple different Bragg wavelengths, the number of sensors can be increased even further (Götten et al., 2020).

While CDM and WDM can be used in optical sensor networks, they originate from data transmission applications, such as cellular and global positioning system (GPS) systems (Lim et al., 2006). WDM is the optical equivalent to frequency-division multiplex (FDM) in data transmission systems. CDM spreads a single transmitted symbol, applying a code sequence. On the receiver side correlation is used to regain the transmitted symbol out of a signal distorted by multiaccess-interference (MAI). With this procedure multiple data transmissions can take place over a single channel (Price and Green, 1958).

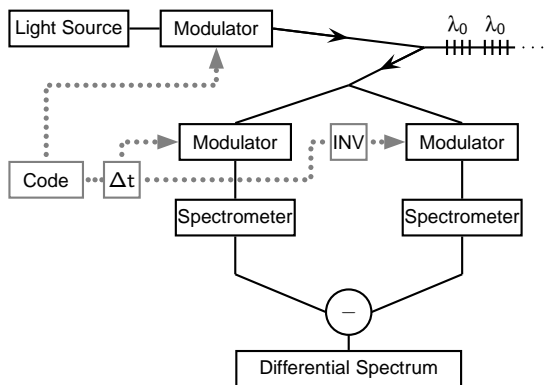


Figure 1: Setup of CDM Interrogation System (Götten et al., 2020).

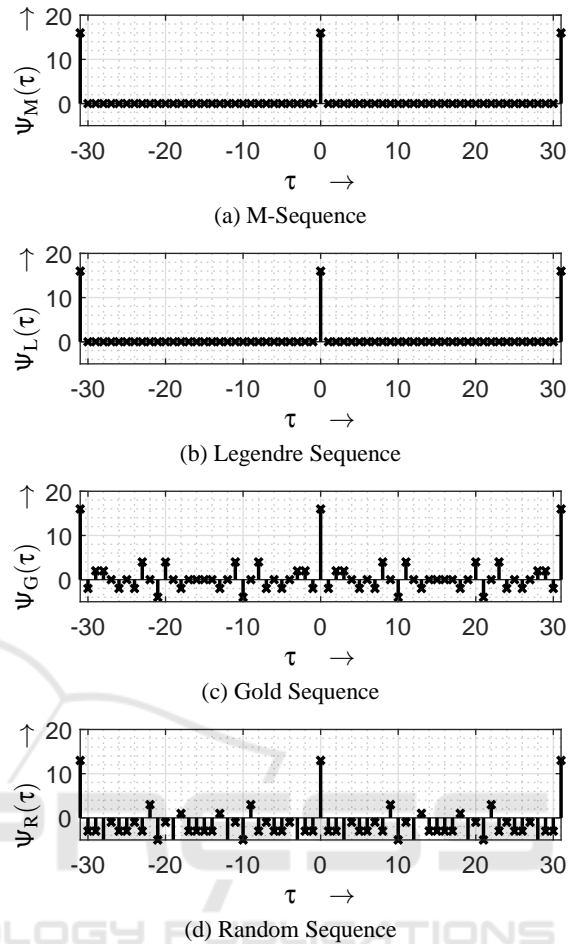


Figure 2: Cyclical autocorrelation function (ACF) obtained applying SIK of different sequence types with a length of 31 chips.

One of the important aspects for CDM is the selected sequence. Since the cross-correlation function (CCF) between sequences, for example for a set of Gold-sequences, is minimal, data can be received asynchronously (Gold, 1967). For the optical sensor application a single code is used to take advantage of the different optical path lengths for different FBG sensors. Together with an advantageous autocorrelation function (ACF) of an applied sequence, this can be used to read out a specific sensor. Due to the different arrival times of the reflected sequences, the time delay for the second set of modulators is crucial. The reflected sequence of the interrogated FBG needs to be synchronous to the modulators, which corresponds to the ACF peak. Hence, all interfering sensors are attenuated with the value of the side lobes.

Thus, the side lobes of the ACFs of each sensor for the optical sensor application, as well as the side lobes of the ACFs of each data transmission have to be investigated, as they can influence the measurement.

Therefore, different sequences shown in Figure (figure 2) are evaluated.

Since binary Legendre and M-sequences provide side lobes of -1 in their cyclical bipolar-bipolar ACF, they are chosen for these particular CDM applications (Boehmer, 1967). By nature, incoherent light can only be turned on and off. The unipolar version of these sequences needs to be used. Applying SIK, their cyclical unipolar-bipolar ACF is calculated, which leads to side lobes with the value zero, as depicted in Figures 2a and 2b. Gold sequences find usage in CDM systems because of their good cross correlation behaviour within a set of Gold sequences. Their cyclical unipolar-bipolar ACF is shown in Figure 2c. Additionally, random sequences with their inherent good orthogonality are investigated, as well. They rely on a statistical process, that has best correlation behaviour only to its identical sequence, as seen in Figure 2d. Gold and random sequences do not provide side lobes with all zero values.

### 3 CODE EVALUATION CRITERIA

As the concept of CDM originates in data transmission applications, the applicable evaluation criteria can be considered. The first criterion, the detection SNR  $\rho$  denotes the squared half worst case vertical eye opening after the correlation  $U_A$  divided by the noise power  $P_N$  applied to the channel

$$\rho = \frac{U_A^2}{P_N} = \frac{(U_S - U_{Int})^2}{P_N}, \quad (1)$$

where  $U_{Int}$  represents the sum of all interferences. For an additive white gaussian noise (AWGN) channel,  $U_A$  is equal to the signal amplitude  $U_S$ . Assuming a time-dispersive channel, intersymbol-interference (ISI) diminish the half vertical eye opening. Considering multiple users in a CDM system, MAI, which is included in  $U_{Int}$ , is subtracted, too. In Figure 3 the relation between combined interferences  $U_{Int}$ ,  $\rho$  and

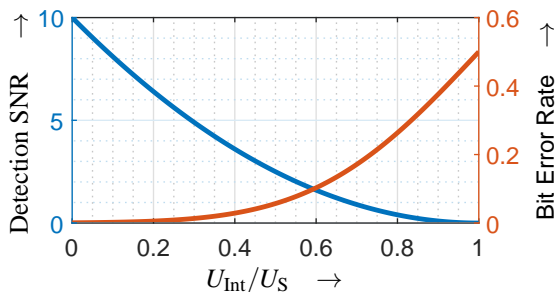


Figure 3: Relation between combined interferences  $U_{Int}$ , detection SNR  $\rho$  and bit error rate (BER)  $P_E$ , assuming  $P_N = 0.1 \text{ V}^2$  and  $U_S = 1 \text{ V}$ .

bit error rate (BER)  $P_E$  is displayed. An optimum of  $\rho = 10$  and  $P_E = 7.8 e^{-4}$  is depicted for no interferences. If  $U_{Int}$  matches  $U_S$ ,  $\rho$  reaches zero, consequently  $P_E$  is at it's maximum 0.5.

The bit error rate (BER)  $P_E$ , which is the second criterion, states the number of falsely transmitted bits, that equal the symbols, the bit errors, divided by the number of all transmitted bits. It is one of the basic criteria to evaluate data transmission systems. For a two level transmission system it can also be estimated by applying the complementary error function (erfc) to the previously defined detection SNR  $\rho$

$$P_E = \frac{1}{2} \text{erfc} \left( \sqrt{\frac{\rho}{2}} \right). \quad (2)$$

Hence, the detection SNR and the BER are suitable criteria for a CDM transmission system.

A corresponding criterion can be considered for the sensor application, derived from  $\rho$ . It is based on the spectral behaviour of a sensor system and depicted in Figure 4. Referring to the high amount of FBGs in an optical sensor network mentioned in Section 1, it is inevitable that multiple sensors operate at the same wavelength, which are distributed in different sections. CDM distinguishes between these sections. The interrogated sensor is referred to as signal, while the rest is considered as positive or negative multiuser-interference (MUI), depending on the applied code. To evaluate the measurand, the wavelength shift of a sensor is analysed. Consequently, the peak wavelength of a sensor can shift according to the applied strain or temperature. This applies to each single sensor in each section  $k$  in the network, so that the interfering sensors can be spectrally shifted, too. Out of all combinations, the worst-case is considered for the criterion. When all positive interference  $MUI_k^+$  is spectrally shifted and all negative interference  $MUI_k^-$  overlaps with the signal from the interrogated sensor  $s_k$ , the signal peak is diminished and in competition with the positive interference. The ratio between the remaining signal peak and the positive

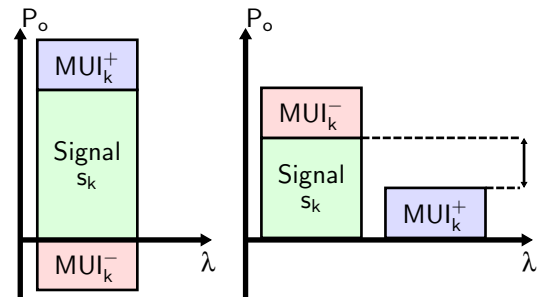


Figure 4: Graphic representation of mSMUI, where  $P_o$  is the spectral optical power density depending on the wavelength  $\lambda$ .

interference is defined as a modified signal-to-MUI ratio  $mSMUI_k$  for section  $k$ . The spectral noise density  $N_0$  can be added to the ratio as well, so that the equation results in

$$mSMUI_k = \frac{s_k - MUI_k^-}{MUI_k^+ + N_0}. \quad (3)$$

Comparing the detection SNR with the  $mSMUI$  it can be seen, that the signal  $U_S$  for data transmission and  $s_k$  for the sensor application are diminished by  $U_{Int}$  or MUI respectively. Due to the possibility of spectral shifting and the need for a worst case consideration, the MUI in the sensor network has to be split into positive and negative parts. In data transmission systems this separation is not required, as interferences affect the detection SNR only at the point of decision at the receiver side. Therefore, interferences can be constructive or destructive for the half vertical eye opening.

#### 4 SENSOR SYSTEM SIMULATION

Based on the previously, in Section 2, explained CDM-WDM system, a simulation is programmed. It is used to provide information about the usability of applied sequences. The simulation is situated on the chip-level, meaning the single logical '1's and '0's of the binary sequence. This automatically includes a rectangular chip shaping that is applied in the mentioned interrogation system. The optical correlation of this system comprises a multiplication step, realized by an optical modulator and a summation step, realized by a spectrometer. This setup needs to be transferred into a mathematical description. The size of the sum, how many chips are summed up, is defined by the integration time of the spectrometer and the duration of each chip. At the beginning of the integration time, the first modulator starts and the light needs to travel through the whole sensor network before it arrives at the second modulator. Depending on the optical path length, the reflected sequence arrives with a different time delay. Besides this sequence, the modulator is synchronized to, interfering reflections arrive sooner and later. Therefore, the modulator is driven with a sequence starting with the beginning of the integration time. To create the appropriate time delay, the sequence is rotated, so that the last chips of the sequence are at the very beginning. To fill the integration time, the sequence is repeated several times and at the end both modulators stop with the actual last chip of the sequence. The integration time is set so that no sequence is truncated

at the end. Instead, the modulators are driven with logical '0's, to fill the remaining integration time. The simulation uses a matrix calculation to obtain the autocorrelation results for each section of the system, assuming the minimum distance of sensors operating at the same wavelength equal to the chip duration. The investigated sequence  $\mathbf{c}$  consists of a certain number of chips  $c_n$  where  $n = 0, 1, \dots, N-1$  and  $N$  denotes the length of the sequence. The arriving sequences with different time delays at the second modulator are represented in the matrix  $\mathbf{S}^{(K \times I)}$  where  $K$  stands for the number of sections and  $I$  for the integration time in chips. The integration time  $I$  needs to be equal to or greater than the length of the sequence  $N$ .

$$\mathbf{S} = \begin{bmatrix} c_0 & \dots & c_{N-1} & 0 & \dots & 0 \\ 0 & \dots & c_{N-2} & c_{N-1} & \dots & 0 \\ \vdots & & \ddots & & & \\ 0 & \dots & 0 & c_0 & \dots & c_{N-1} \end{bmatrix} \quad (4)$$

The delay is implemented on the chip level by adding zeros in front of the first sequence. For each section an additional zero indicates an additional time delay matching the distance of sensors at the same wavelength. The sequence itself is repeated to fill the integration time  $I$ . No sequence is truncated. Instead, zeros fill the remaining columns of the matrix. Thus, all sequences from different sections, meaning with different time delays, are represented in the matrix  $\mathbf{S}$ . The behavior of the second modulator is defined in matrix  $\mathbf{R}^{(K \times I)}$ . Instead of the leading zeros for the time delay, the matrix is filled with rotated parts of the sequence. Therefore the last chips of a sequence appear in front of the first chip.

$$\mathbf{R} = \begin{bmatrix} c_0 & \dots & c_{N-1} & 0 & \dots & 0 \\ c_{N-1} & \dots & c_{N-2} & c_{N-1} & \dots & 0 \\ \vdots & \ddots & & & & \\ c_1 & \dots & c_0 & c_1 & \dots & c_{N-1} \end{bmatrix} \quad (5)$$

This matrix realizes each synchronization point, thus each possible time delay for the simulated network. The integration time here is filled with zeros at the end, as well. Each element in one line of the matrix  $\mathbf{S}$  needs to be multiplied with the corresponding element of each line of the matrix  $\mathbf{R}$ . All these elements need to be summed up to fulfill the correlation of both sequences. This happens line-wise and can be realized by a matrix multiplication

$$\mathbf{A} = \mathbf{S} \cdot \mathbf{R}^T. \quad (6)$$

The matrix  $\mathbf{A}^{(K \times K)}$  contains all correlation functions for each section in its lines. All side lobes can be assigned to the corresponding section and the ACF

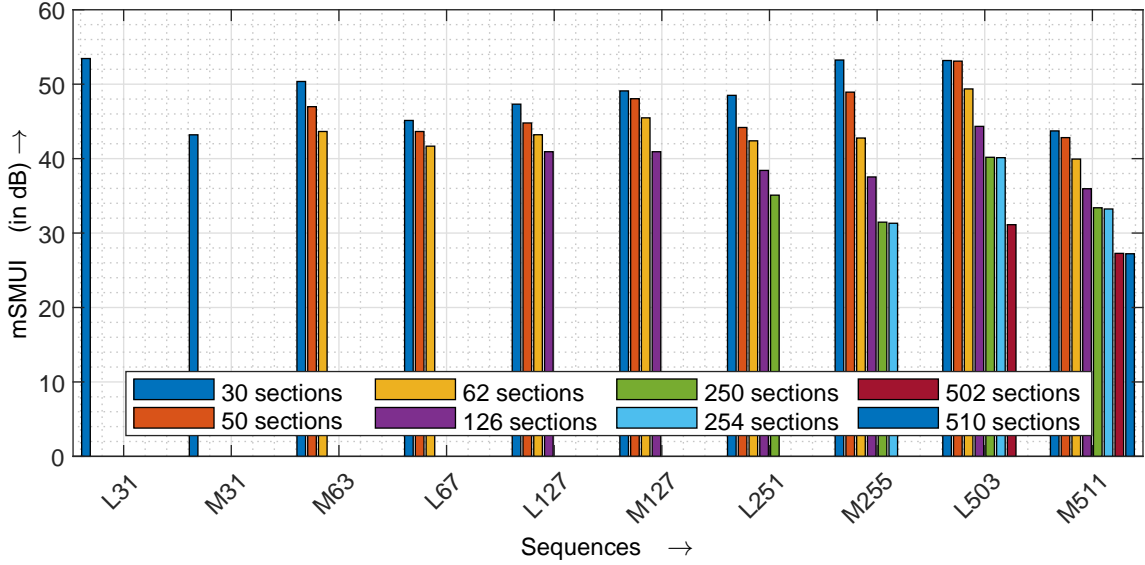


Figure 5: Simulated mSMUI as a function of selected code sequences and network size (with reference to Table 1).

peaks can be found along the main diagonal. Hence, the vector  $\mathbf{s}$  contains all ACF peaks

$$\mathbf{s} = (a_{0,0}, a_{1,1}, \dots, a_{K-1,K-1}), \quad (7)$$

whereas the matrix  $\mathbf{M}^{(K \times K)}$

$$\mathbf{M} = \mathbf{A} - \text{diag}(\mathbf{s}) \quad (8)$$

contains all interference between each section. The interference of section  $j$  on section  $k$  is indicated by the matrix element  $m_{k,j}$ . Consequently, all elements on the main diagonal are zero, since there cannot be an interference of a section on itself. The interference can be positive or negative, so that the separate sums of all positive and of all negative interference for each section  $k$  are calculated by

$$\text{MUI}_k^+ = \sum_j m_{k,j} \quad \forall j \in \{0, 1, \dots, K-1 | m_{k,j} > 0\}, \quad (9)$$

$$\text{MUI}_k^- = \sum_j |m_{k,j}| \quad \forall j \in \{0, 1, \dots, K-1 | m_{k,j} < 0\}. \quad (10)$$

The corresponding signal  $s_k$  of the section  $k$  is an element in vector  $\mathbf{s}$ . Thus, signal, positive interference and negative interference are calculated and can be used for determining the criteria  $\text{mSMUI}_k$  to evaluate the sequence  $\mathbf{c}$ . This  $\text{mSMUI}_k$  is section and integration time dependent. The integration time defines the number of repetitions of the sequence  $\mathbf{c}$  and the amount of zeros in the last columns of matrix  $\mathbf{S}$  and matrix  $\mathbf{R}$ . Non-cyclical ACFs contain boundary effects at the beginning and at the end of the sequence. In contrary, the cyclical ACF attained with SIK for M-sequences and Legendre sequences contains zeros for

all side lobes. Meaning, for every additional repetition of the sequence, the signal  $s_k$  increases while the interference stays the same. Therefore, the worst-case criterion  $\text{mSMUI}_k$  can be improved by additional repetitions. In the testbed they are limited by the integration time of the spectrometer. Hence, the simulation can calculate the criterion for a few repetitions of the sequence  $\mathbf{c}$  and the results can be scaled to the corresponding integration time. The scaling only applies when a full repetition is added. Therefore, the simulation calculates all  $\text{mSMUI}_k^{(I)}$  for each section  $k$  and for each integration time  $I$  until another repetition fits inside without truncating the sequence. Out of these results the worst  $\text{mSMUI}_k^{(I)}$  is considered for the evaluation of the sequence  $\mathbf{c}$ .

The simulation parameters are depicted in Table 1. The chip duration  $T_c$  equals 5 ns which corresponds to a distance of 1 m between two sensors operating at the same wavelength (Götten et al., 2020). The integration time is set from 13000 chips to 13000 +  $N$  chips, where  $N$  indicates the length of the sequence. Thus, all boundary effects resulting in interference are considered for the mSMUI. The actual integration time can be calculated by multiplying the amount of chips

Table 1: Simulation parameters.

Parameter	Value
Chip duration $T_c$	5 ns
Scaling factor	$\times 100$
Integration time	13000 ... 13000 + $N$ chips
Resulting I-time	6.5 ms ... 6.5 ms + $N \cdot T_c$
Number of sections	30 ... 510 sections

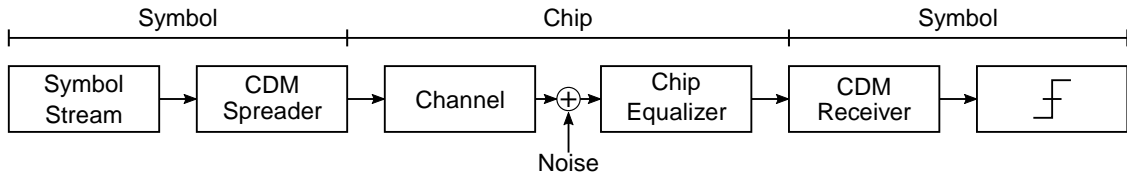


Figure 6: Simulation of data transmission using a single user CDM system.

with  $T_c$  that results in  $6.5 \mu\text{s}$  for 13000 chips. Measurements with the interrogator testbed show integration times of  $\sim 6.5 \text{ ms}$ . Therefore, a scaling factor of  $\times 100$  is chosen to correspond to actual measurements. The number of sections varies from 31 to 510. It is chosen to exhaust the maximum coverage of the investigated sequences which is one section less than the length  $N$ . 50 serial WDM sections have already been interrogated in the testbed. The analyzed sequences range from suitable Legendre sequences with the lengths from 31 to 503 chips (L31 – L503) and M-sequences ranging from 31 to 511 chips (M31 – M511). In the case of M-sequences, all possible sequences with different generator polynomials are analyzed. Gold and random sequences are not depicted since they provide side lobes in their cyclical ACF that lead to a very low mSMUI.

Figure. 5 depicts the simulation results. The criterion is represented in the dB-scale, since possible negative ratios (when  $s_k < \text{MUI}_k^-$ ) can be excluded and set to 0 dB. The dependency of the maximum coverage on the sequence length can be seen by the amount of sections each sequence can handle. The scenario for 30 sections leads to results for all tested sequences. 50 sections are not supported by sequence lengths of 31 chips. The more sections, the longer the sequence has to be. The number of repetitions of a sequence does not influence the mSMUI. Sequence L31 provides an mSMUI of 53.45 dB for 30 sections. Sequences M255 and L503 reach similar values, while the rest is lower. Whereas the Legendre sequence L31 in the 30 sections scenario provides better results than the M-sequence M31, no general rule for Legendre and M-sequences can be found. For complete coverage and equal lengths, the Legendre sequence L31 is superior to M31 and L127 is equal to M127. L503 seems to be an all-rounder for all simulated scenarios. It has no major drawback for a small amount of sections and is superior for all numbers of sections until complete coverage of 502 sections. The interrogation of such a network length suffers from other influences that cannot be improved by the sequence itself (Götten et al., 2020).

## 5 DATA TRANSMISSION SYSTEM SIMULATION

The simulation of data transmission describes a single user CDM system, since ISI is the equivalent to the MUI in the sensor system and therefore, a better comparability is achieved. Included are a binary generator, a CDM spreader and receiver, a pair of root-raised cosine filters, a chip level equalizer and a frequency selective channel with noise influence. An overview is provided in Figure 6. The binary generator provides a bipolar '1', '-1' symbol stream. The CDMA spreader increases the required bandwidth, by spreading each transmitted data symbol with a specific sequence. The CDM receiver works by correlating the received signal with the original sequence. Channel coefficients and noise can be individually defined. The equalizer works on chip level (Darwood et al., 2001), (Elders-Boll, 2001). After the CDM receiver, evaluation mechanisms are used to assess the received signal. These mechanisms include a decider, which converts the received signal back into symbols, and a comparison of received and transmitted symbol stream.

The channel impulse response  $g_c(t)$  is given with

$$g_c(t) = g_0 \cdot \delta(t) + g_1 \cdot \delta(t - T_S) + g_2 \cdot \delta(t - 1.5T_S). \quad (11)$$

The channel coefficients are selected with  $g_0 = 0.8578$ ,  $g_1 = 0.4289$  and  $g_2 = 0.2831$ , so that the channel impulse response is power neutral.

The compared codes include M-sequences, Legendre-sequences, Gold-sequences and random sequences with the length of 31 and 127 chips. Furthermore, an example of M-sequences with a length of 15 and 63 chips are tested. The noise is given through the energy per bit to noise power spectral density ratio  $10 \cdot \lg(E_S/N_0)$  with 10 dB. As this simulation is describing a single user system, the MAI, mentioned in Section 3, is set to zero. Every simulation was done with and without the application of a chip level equalizer.

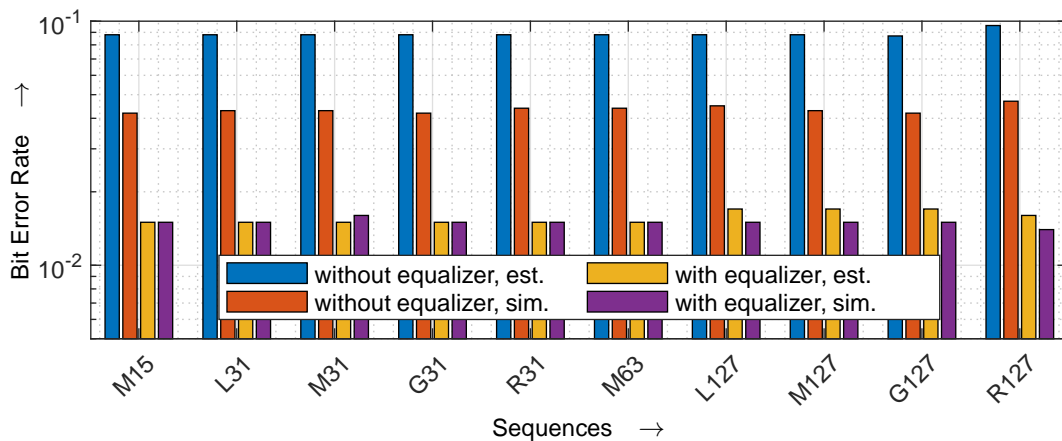


Figure 7: Simulated BER as a function of selected code sequences with an SNR  $10 \cdot \log_{10}(E_s/N_0)$  of 10 dB.

The results are shown in Figure 7. For the simulations without equalizer it is shown, that the calculated values are about half of the simulated values. This is explained by taking into account, that the calculation assumes the worst case half vertical eye opening, while the simulation includes all possible half vertical eye openings. This difference changes, for the simulations with equalizer, as it sets all half vertical eye openings near to the value of 1 V. It can be seen, that over all sequences the BER  $P_E$  for the respective set ups and calculations is similar.

The channel coefficient  $g_2$  is multiplied by the corresponding side lobe of the ACF, which affects the half vertical eye opening. This explains the differences in results for estimated values for G127 and R127 without equalizer. Simulated results are subject to statistical processes, such as symbol stream generation and noise application. With the inclusion of the equalizer into the estimation, the values are the same for all sequences up to the length 63. The half vertical eye opening for these sequences is set to 1 V. As the half vertical eye opening drops slightly for the sequences with a length of 127, down to 0.98 V for M-, Legendre- and Gold sequences and 0.985 V for the random sequence,  $P_E$  is slightly worse for the same amount of equalizer coefficients.

## 6 CONCLUSION

In this work three system based code evaluation criteria are introduced. The main difference between data transmission and sensor applications is the handling of interferences. For data transmission applications, the worst half vertical eye opening caused by all interferences is considered to estimate the criteria. The worst case criteria for the sensor application is not a

superposition of all influences, but a separate evaluation of positive and negative MUI. Different sequences result in different mSMUI and the sequence length defines the maximum number of sections, that can be interrogated. While the ACF obtained by SIK of Legendre- and M-sequences provides zero values for all side lobes, Gold- and random sequences show non-zero values and are therefore not applicable. The Legendre sequence with a length of 503 chips shows an overall best result. In contrary, in the proposed single user CDM system the spreading sequence shows no major influence.

## ACKNOWLEDGEMENTS

This work has been funded by the German Ministry of Education and Research (No. 13FH030PX8).

## REFERENCES

- Boehmer, A. (1967). Binary pulse compression codes. *IEEE Transactions on Information Theory*, 13(2):156–167.
- Braghin, F., Cazzulani, G., Cinquemani, S., and Resta, F. (2013). Potential of FBG Sensors for Vibration Control in Smart Structures. In *2013 IEEE International Conference on Mechatronics (ICM)*. IEEE.
- Darwood, P., Alexander, P., and Oppermann, I. (2001). LMMSE chip equalisation for 3GPP WCDMA downlink receivers with channel coding. In *ICC 2001. IEEE International Conference on Communications. Conference Record (Cat. No.01CH37240)*, volume 5, pages 1421–1425 vol.5.
- Elders-Boll, H. (2001). “performance of an adaptive lmmse chip equalizer for ultra-fdd downlink detection. In *Proc. COST 262 Workshop*, pages 1–6.

- Gold, R. (1967). Optimal Binary Sequences for Spread Spectrum Multiplexing (Corresp.). *IEEE Transactions on Information Theory*, 13(4):619–621.
- Götten, M., Lochmann, S., Ahrens, A., Lindner, E., and Roosbroeck, J. V. (2020). 2000 Serial FBG Sensors Interrogated With a Hybrid CDM-WDM Scheme. *Journal of Lightwave Technology*, 38(8):2493–2503.
- Götten, M., Lochmann, S., Ahrens, A., and Benavente-Peces, C. (2020). A Robust Serial FBG Sensor Network with CDM Interrogation allowing Overlapping Spectra. In *Proceedings of the 9th International Conference on Sensor Networks*. SCITEPRESS - Science and Technology Publications.
- Jelbuldina, M., Korobeinyk, A., Korganbayev, S., Tosi, D., Dukenbayev, K., and Inglezakis, V. J. (2018). Real-Time Temperature Monitoring in Liver During Magnetite Nanoparticle-Enhanced Microwave Ablation With Fiber Bragg Grating Sensors: Ex Vivo Analysis. *IEEE Sensors Journal*, 18(19):8005–8011.
- Kaplan, N., Jasenek, J., Cervenova, J., and Usakova, M. (2019). Magnetic Optical FBG Sensors Using Optical Frequency-Domain Reflectometry. *IEEE Transactions on Magnetics*, 55(1):1–4.
- Lim, K., Lee, S. ., Min, S., Ock, S., Hwang, M. ., Lee, C. ., Kim, K. ., and Han, S. (2006). A fully integrated direct-conversion receiver for cdma and gps applications. *IEEE Journal of Solid-State Circuits*, 41(11):2408–2416.
- Nawrot, U., Geernaert, T., Pauw, B. D., Anastasopoulos, D., Reynders, E., Roeck, G. D., and Berghmans, F. (2017). Mechanical strain-amplifying transducer for fiber Bragg grating sensors with applications in structural health monitoring . In Chung, Y., Jin, W., Lee, B., Canning, J., Nakamura, K., and Yuan, L., editors, *25th International Conference on Optical Fiber Sensors*. SPIE.
- Ou, Y., Zhou, C., Qian, L., Fan, D., Cheng, C., Guo, H., and Xiong, Z. (2017). Large WDM FBG Sensor Network Based on Frequency-Shifted Interferometry. *IEEE Photonics Technology Letters*, 29(6):535–538.
- Presti, D. L., Massaroni, C., D'Abbraccio, J., Massari, L., Caponero, M., Longo, U. G., Formica, D., Oddo, C. M., and Schena, E. (2019). Wearable System Based on Flexible FBG for Respiratory and Cardiac Monitoring. *IEEE Sensors Journal*, 19(17):7391–7398.
- Price, R. and Green, P. (1958). A Communication Technique for Multipath Channels. *Proceedings of the IRE*, 46(3):555–570.
- Rajan, G., editor (2015). *Optical Fiber Sensors: Advanced Techniques and Applications*. CRC PR INC.
- Wang, Y., Gong, J., Dong, B., Wang, D. Y., Shillig, T. J., and Wang, A. (2012). A Large Serial Time-Division Multiplexed Fiber Bragg Grating Sensor Network. *Journal of Lightwave Technology*, 30(17):2751–2756.